# Analysis of High Frequency Characteristics for a Meander Line Slow-wave Structure


***Zheng Wen[1,2], Jirun Luo[1,2], Yu Fan[1,2], Chen Yang[1,2], Fang Zhu[2], Min Zhu[2], Wei Guo[2], Yubin Gong[3], and Jinjun Feng[4]***

[1]Key Laboratory of High Power Microwave Source and Technologies, Institute of Electronics, Chinese Academy of Sciences, Beijing 100190, China

[2]University of Chinese Academy of Sciences, Beijing 100049, China

[3]National Key Laboratory of Science and Technology on Vacuum Electronics, University of Electronic Science and Technology of China, Chengdu, 610054, China

[4]Vacuum Electronics National Laboratory, Beijing Vacuum Electronics Research Institute, Beijing, 100016, China

Contact Author Email: wenzheng17@mails.ucas.edu.cn



**Abstract:** *Analysis of high frequency characteristics for a meander line slow-wave structure (ML-SWS) has been carried out by field-matching methods with the dyadic Green's function. The effect from thickness of the meander line was considered and the theoretical results had been compared with the simulation ones.*



**Keywords:** Meander line; slow-wave structure; traveling wave tube (TWT); dyadic Green's function; field-matching methods.


## Introduction

Owing to the traditional slow-wave structure (SWS), the core of the TWT, is difficult to be fabricated by conventional fabrication technologies, with the operation frequency moving to Ka-band or above [1]. A new type of the SWS, the meander line slow-wave structure, compatible with the microfabrication technologies, comes into being [2]. To the best of our knowledge, the most analyses of the ML-SWS are exclusively with numerical simulations [2-3], and the few theoretical analyses are based on ignoring the thickness of the ML [4-5].

## Model and Results

The ML-SWS consists of the meander line and Rectangular waveguide as shown in figure 1. For lossless system, the model can be simplified with just one period of the ML-SWS, according to Fouquet's theorem. The electrical field as source can excite the magnetic fields, $\vec{H}_{RW}$ in the rectangular waveguide, and $\vec{H}_{ML}$ in the meander line, respectively. They satisfy the field-matching equation as:

$$\vec{H}_{RW}(\vec{R}) = \vec{H}_{ML}(\vec{R}), \vec{R} \in \text{Meander-Line} \tag{1}$$

The magnetic field can be described with the equivalent electrical field by the following equation:

$$\vec{H}\left(\vec{R}\right) = -i\omega\varepsilon_0 \int_{S'} \vec{\vec{G}}\left(\vec{R},\vec{R}'\right) \cdot \left(\hat{n} \times \vec{E}\left(\vec{R}'\right)\right) dS' \tag{2}$$

where $\vec{E}\left(\vec{R}'\right)$ is the equivalent electrical fields and $\vec{\vec{G}}\left(\vec{R},\vec{R}'\right)$ is the dyadic Green's function, and the $\vec{E}\left(\vec{R}'\right)$ can be written with sets of Ritz basic functions $\{\varphi_n\}$, which are shown as below:

$$\vec{E} = \sum_n A_n \varphi_n \tag{3}$$

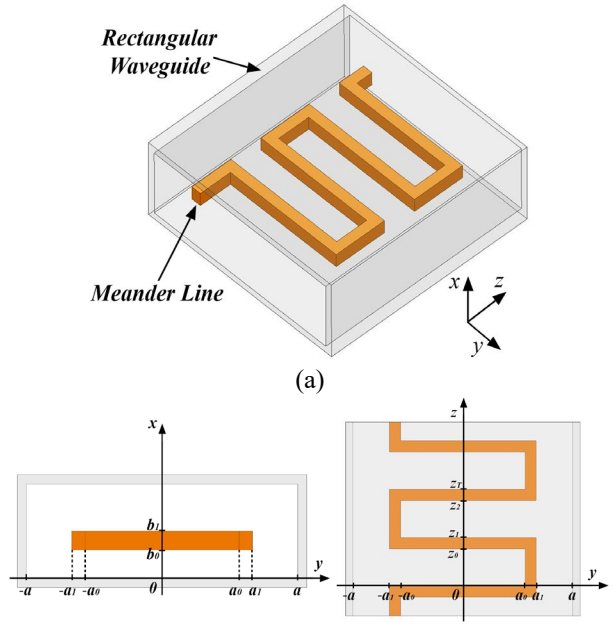


**Figure 1.** Geometry of the ML-SWS. (a) 3D model view, (b) front view, (c) top view.

The Ritz basic functions $\{\varphi_n\}$ can be obtained according to [6]. For instance, the $\varphi_n$ in x-axis direction can be written:

$$\varphi_n = \hat{x}\cos\left(n\pi\left(x - b_0\right)/\left(b_1 - b_0\right)\right) \tag{4}$$

The dyadic Green's function $\vec{\vec{G}}$ can be divided into two part, $\vec{\vec{G}}_T$ for the sum of "TE" and "TM" modes, and $\vec{\vec{G}}_{TEM}$ for the "TEM" mode.

$$\vec{\vec{G}} = \vec{\vec{G}}_T + \vec{\vec{G}}_{TEM} \tag{5}$$

where $\vec{\vec{G}}_T$ and $\vec{\vec{G}}_{TEM}$ can be written as following:

$$\vec{\vec{G}}_T = \frac{1}{V_{\text{out}}} \sum_{\kappa} \left( \frac{\left(2-\delta_{k_c}\right)\left(\nabla\times\left(\vec{C}\cdot f_M(x,y,z)\right)\right)\left[\left[\nabla\times\left(\vec{C}\cdot f_M(x',y',z')\right)\right]\right]^*}{\left(k_c\right)^2\left(\left(\kappa\right)^2 - k^2\right)} + \frac{\left(2-\delta_{k_c}\right)\left(\nabla\times\nabla\times\left(\vec{C}\cdot f_N(x,y,z)\right)\right)\left[\left[\nabla\times\nabla\times\left(\vec{C}\cdot f_N(x',y',z')\right)\right]\right]^*}{\left(k_c\right)^2\left(\kappa\right)^2\left(\left(\kappa\right)^2 - k^2\right)} \right) \tag{6}$$

$$\overrightarrow{\overrightarrow{G}}_{TEM}^{l}=\begin{cases}\dfrac{3\sum\limits_{s}\dfrac{1}{\left(h_0^2-k^2\right)}\begin{pmatrix}\hat{x}\left(x-x_s^l\right)e^{ih_0z}\\-\hat{y}\left(y-y_s^l\right)e^{ih_0z}\end{pmatrix}\begin{pmatrix}\hat{x}\left(x-x_s^l\right)e^{-ih_0z'}\\-\hat{y}\left(y-y_s^l\right)e^{-ih_0z'}\end{pmatrix}}{2V_l\left(\left(x_t^l-x_s^l\right)^2+\left(y_t^l-y_s^l\right)^2\right)}\\ \dfrac{3\sum\limits_{s}\dfrac{1}{\left(h_0^2-k^2\right)}\begin{pmatrix}-\hat{x}\left(x-x_s^l\right)e^{ih_0y}\\\hat{z}\left(z-z_s^l\right)e^{ih_0y}\end{pmatrix}\begin{pmatrix}-\hat{x}\left(x-x_s^l\right)e^{-ih_0y'}\\\hat{z}\left(z-z_s^l\right)e^{-ih_0y'}\end{pmatrix}}{2V_l\left(\left(x_t^l-x_s^l\right)^2+\left(z_t^l-z_s^l\right)^2\right)}\end{cases} \quad (7)$$

Hence, considering the superposition principle, the field-matching equation can be rewritten with the matrix form:

$$[Y][A]=0 \quad (8)$$

where the matrix $[A]$ is a set of variables $\{A_n\}$. In fact, it is also a vector. The matrix $[Y]$ can be expressed by variables $\omega$ and $\theta$. The nonzero solution exists only if the value of corresponding determinant $|Y|$ is zero.

Accordingly, the dispersion characteristic equation is obtained as following:

$$|Y|=0 \quad (9)$$

In addition, according to equation (8), the variable $A_n$ can be solved for concrete frequency $\omega_0$ and phase shift $\theta_0$, namely, $A_n|_{\omega_0,\theta_0}$. Considering no exciting source, the electro-magnetic field in the ML-SWS can be obtained:

$$\begin{cases}\vec{H}_{\text{out}}(\vec{R})\big|_{\omega_0,\theta_0}=-i\omega_0\varepsilon_0\sum\limits_{n}\left(A_n|_{\omega_0,\theta_0}\int_{S'}\overrightarrow{\overrightarrow{G}}\left(\vec{R},\vec{R}'\right)\cdot\left(\hat{n}\times\varphi_n\right)dS'\right)\\ \vec{E}_{\text{out}}(\vec{R})\big|_{\omega_0,\theta_0}=-\left(\nabla\times\vec{H}_{\text{out}}(\vec{R})\big|_{\omega_0,\theta_0}\right)\Big/\left(i\omega_0\varepsilon_0\right)\end{cases} \quad (10)$$

The interaction impedance $R_{\omega_0,\theta_0}$ can be calculated:

$$R_{\omega_0,\theta_0}=\left|\vec{E}_{\text{out}}(\vec{R})\big|_{\omega_0,\theta_0}\right|^2\Big/\left(2\beta_{\omega_0,\theta_0}^2P\right) \quad (11)$$

where $P$ is the total power, $\beta_{\omega_0,\theta_0}=\left(\theta_0+2s\pi\right)/T$, $T$ is the length of a period.

Here, an example is calculated, and the parameters of the ML-SWS are exhibited in Table 1:

**Table 1.** The parameters of the ML-SWS (mm)

| | | | | |
|---|---|---|---|---|
| b=3 | $b_0$=1 | $b_1$=1.4 | a=3 | $a_0$=2.2 |
| $a_1$=2.5 | $z_0$=0.3 | $z_1$=1.3 | $z_2$=1.6 | $z_T$=2.6 |

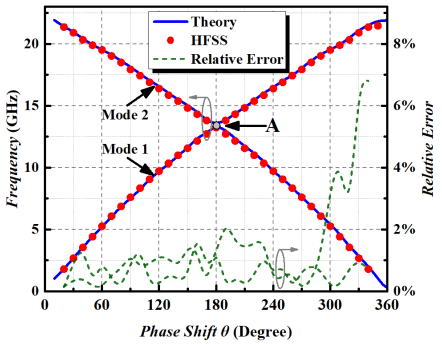


**Figure 2.** Comparison of dispersion of a ML-SWS.

As shown in figure 2. The dispersion results carried out by the proposed method were compared with those simulated with HFSS code, the relative errors between them is under 7%, which demonstrates that the theoretical results and simulated ones are in good agreement.

In figure 2 and 3, the dispersion of mode 1 is very close to that of mode 2 at point A. As shown in figure 3. When $z_2$=1.6 mm and $z_2$=2.0 mm, there is obvious band gap between the dispersions of adjacent two modes. When $z_2$=2.3 mm, the corresponding structures and sizes of two half-period of the ML are same, and dispersions of two modes are very close to each other near point A, i.e., the band gap seems to disappear.

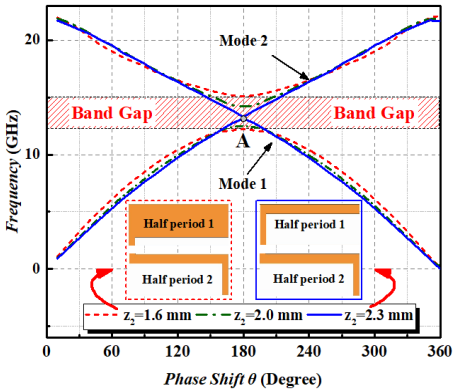


**Figure 3.** Effect of a parameter $z_2$ on the dispersion of the ML-SWS.

## Conclusions

For analyzing the high frequency characteristics of the ML-SWS, the field-matching method with the dyadic Green's function has been utilized in this paper. The theoretical and HFSS simulated results were compared, the relative errors in presented range are under 7%. The band gap of the dispersions may disappear when the corresponding structures and sizes of two half-period of the ML are same for the adjacent two slow wave modes. The more results and analysis will be presented on the conference.

## References


1. L. W. Liu, et al., "A Novel Winding Microstrip Meander-Line Slow-Wave Structure for V-Band TWT," IEEE Electron Device Lett., vol. 34, no. 10, pp. 1325-1327, 2013.
2. N. F. Bai, M. Shen, and X. H. Sun, "Investigation of Microstrip Meander-Line Traveling-Wave Tube Using EBG Ground Plane," IEEE Trans. Electron Devices, vol. 62, no. 5, pp. 1622-1627, 2015.
3. F. Shen, et al., "140-GHz V-Shaped Microstrip Meander-Line Traveling Wave Tube," J. Electromagn. Waves and Appl., vol. 26, pp. 89-98, 2012.
4. F. -J. Glandorf and I. Wolff, "A Spectral-Domain Analysis of Periodically Non-uniform Coupled Microstrip Lines," IEEE Trans. Microw. Theory Tech., vol. 36, no. 3, pp. 522-528. 1988.
5. D. G. Zhang, et al., "Dispersion Characteristics of a novel Shielded Periodic Meander Line," Microw. Opt. Technol. Lett., vol. 12, no. 1, pp. 1-5, 1996.
6. Q. C. Su, and H. S. Wu, "Green's Function Solution of the Waveguide with Two Pairs of Double Ridges," Acta Electronica Sin., vol. 11, no. 5, pp. 81-87, 1983.